Verwey transition in a magnetite ultrathin film by resonant x-ray scattering

S. Grenier, A. Bailly, A. Y. Ramos, M. De Santis, Y. Joly, J. E. Lorenzo, S. Garaudée, M. Frericks, S. Arnaud, N. Blanc, and N. Boudet

Univ. Grenoble Alpes, CNRS, Grenoble INP, Institut Néel, 38000 Grenoble, France

(Received 4 January 2018; revised manuscript received 19 February 2018; published 2 March 2018)

We report a detailed study of the Verwey transition in a magnetite ultrathin film (UTF) grown on Ag(001) using resonant x-ray scattering (RXS). RXS was measured at the Fe K-edge on the crystal truncation rod of the substrate, increasing the sensitivity to the film thanks to the cross-interference, thereby obtaining an x-ray phase-shift reference and a polarization analyzer. The spectra were interpreted with *ad hoc* calculations based on density functional theory within a surface-scattering formalism. We observed that the UTF has a relatively sharp transition temperature $T_V = 120$ K and is remarkably close to the bulk temperature for such thickness. We determined the specific Fe stacking at the interface with the substrate below T_V, and detected a spectroscopic signal evolving with temperature from T_V up to at least $T_V + 80$ K, hinting that the RT crystallographic structure does not set at T_V in the UTF.

DOI: 10.1103/PhysRevB.97.104403

I. INTRODUCTION

The alteration of bulk properties in ultrathin films (UTF) is of interest for device integration and fundamental research, while driving progress in growth engineering. In UTF, interfacial effects like charge transfer or substrate strain on the lattice structure become particularly prominent in materials where charge and orbital orderings, and associated atomic superstructures, underlie sudden transitions in conductivity and magnetism. One material of choice to address this question is magnetite (Fe_3O_4), being the prototype for metal-insulator transition driven by charge ordering and whose growth as UTF has seen recent progress in quality [1–3]. Bulk magnetite is semimetallic but turns into an insulator when cooled down below $T_V = 123$ K, undergoing a sudden electron localization and spatial ordering of ionic Fe^{3+} and Fe^{2+} species, the so-called Verwey transition [4]. Such ordering involving only a fraction of electrons is difficult to extract from the crystal structure as it relies on tabulated cationic volumes assuming ionic features, the structure itself being particularly difficult to determine [5–8]. To circumvent this difficulty, resonant x-ray diffraction (RXD), a spectroscopy-by-diffraction technique, had been used to directly probe the actual Fe charge-ordering layout and the magnitude of the charge modulation [9,10]. RXD relies on the differentiation of the absorption edges, mostly shifted apart, for different charge states of a chemical species, in this case Fe^{2+} and Fe^{3+}. The scattering factors around the edge vary then substantially, $f_{Fe^{2+}}(E) \neq f_{Fe^{3+}}(E)$. By selecting Bragg reflections, Q_{CO}, where the form factor of each one of the charge states has opposite sign, $F(Q_{CO},Fe^{2+}) \sim -F(Q_{CO},Fe^{3+})$, the RXD spectra will be proportional to $|f_{Fe^{2+}} - f_{Fe^{3+}}|^2$. The fingerprint of charge order in the RXD energy scan takes the form of sharp up-and-down anomalies at Q_{CO} and in the neighborhood of the absorption edge. In bulk magnetite, the modeling of the RXD data resulted in a nonionic, multivalent, charge ordering layout with a charge disproportionation of 0.2 electrons [11,12]. In UTF magnetite, a remarkable increase of T_V was observed on a tensile substrate, albeit with an abrupt decrease of T_V from 20 nm down to 2.5 nm-thick UTF [3]. Conventional crystallography would be challenging in these UTF, in addition to lacking the depth sensitivity to charge-ordering variations, but the RXD technique can benefit from the enhancement of the sensitivity to the chemical species layout, as already demonstrated in thick charge-ordered films [13]. In this context, we investigated a magnetite UTF, that we had successfully grown on a silver substrate.

We report here on the detection of the Verwey transition in a UTF 7.4 nm thick, or 8.75 room temperature (RT) unit cells, by detecting its fingerprint on the Fe K-edge RXD spectra. In lack of the sufficient flux to conduct typical RXD measurements, the signal was instead measured using a surface-sensitive methodology [14], in the particular regime of resonant scattering [15], in the sample crystal truncation rod (CTR), taking advantage of the interference between the thickness-limited film and the semi-infinite substrate scattering. This methodology turned out to offer specific information, in particular on the Fe valent state stacking at the interface and on a thermal evolution detected well above T_V.

II. EXPERIMENT

The film was grown by molecular beam epitaxy on a (001)-oriented Ag substrate following a three-step method detailed in Ref. [2]. The epitaxial growth results in a compressive stress which induces a slight tetragonal distortion. For the present *ex situ* study, the magnetite film was covered by a Au protecting layer about 2 nm thick. The surface resonant x-ray diffraction (SRXD) measurements were conducted on the D2AM beamline at the European Synchrotron Radiation Facility. The x-ray beam energy was selected by a double Si(111) crystal monochromator with a 1.5 eV energy bandwidth, and was calibrated at the Fe K-edge with the absorption of a pure Fe foil

 ©2018 American Physical Society

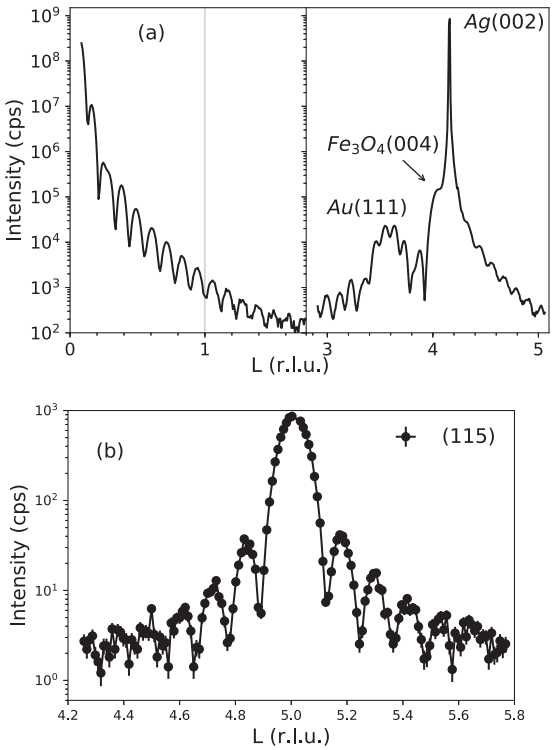

FIG. 1. (a) Scattering along the $Q = (00L)$ direction (in relative lattice unit of the magnetite UTF), showing the substrate, the magnetite layer, and the Au cap layer on the same intensity scale with 7.112 keV photon energy at 40 K. (b) Magnetite UTF (115) reflection on which the thickness was evaluated at 8.75 unit cell, 74 Å (a guiding line connects the data points).

(the maximum derivative was set to 7112 eV); we estimated the accuracy and the precision to be 0.3 eV and 0.05 eV, respectively. In contrast to measurements on bulks, spectral corrections due to self-absorption are negligible. Fluorescence from the magnetite UTF was about 10 counts/s on the largest integration area of the 2D detector. Maximum of its first derivative was near 7123.5 eV. The incident polarization and the scattering plane were kept perpendicular (the so-called σ polarization). Intensity was measured using an XPAD camera, the spectra presented are integrated areas. A commercial He Displex cryostat was used to cool the sample down to 40 K, with a temperature accuracy better than 1 K.

Figure 1 (a) shows the Ag substrate CTR measured at 40 K and its (002) Bragg reflection. The Kiessig fringes from the magnetite film and its (004) Bragg reflection, and the Au cap layer (111) Bragg reflection are observed. The Au (222) was also observed (not shown), with no Kiessig fringes, it thus has a large roughness, potentially with a 3D morphology, thus all the Kiessig fringes correspond to the magnetite thickness, mainly. For magnetite, in addition to the (004), we measured the (008), the (115) shown in Fig. 1(b), and the (444) Bragg reflections. Supposing a tetragonal structure, the (008) reflection gives $c = 8.454(1)$ Å, which is used to estimate $a = 8.29(1)$ Å from the (115) reflection. The Kiessig fringes on the (115) give a thickness of nearly 74 Å, that is 8.75 of the RT unit cell (a .75 unit cell is a unit cell lacking two planes of Fe). The film is thus of high quality with well-defined thicknesses.

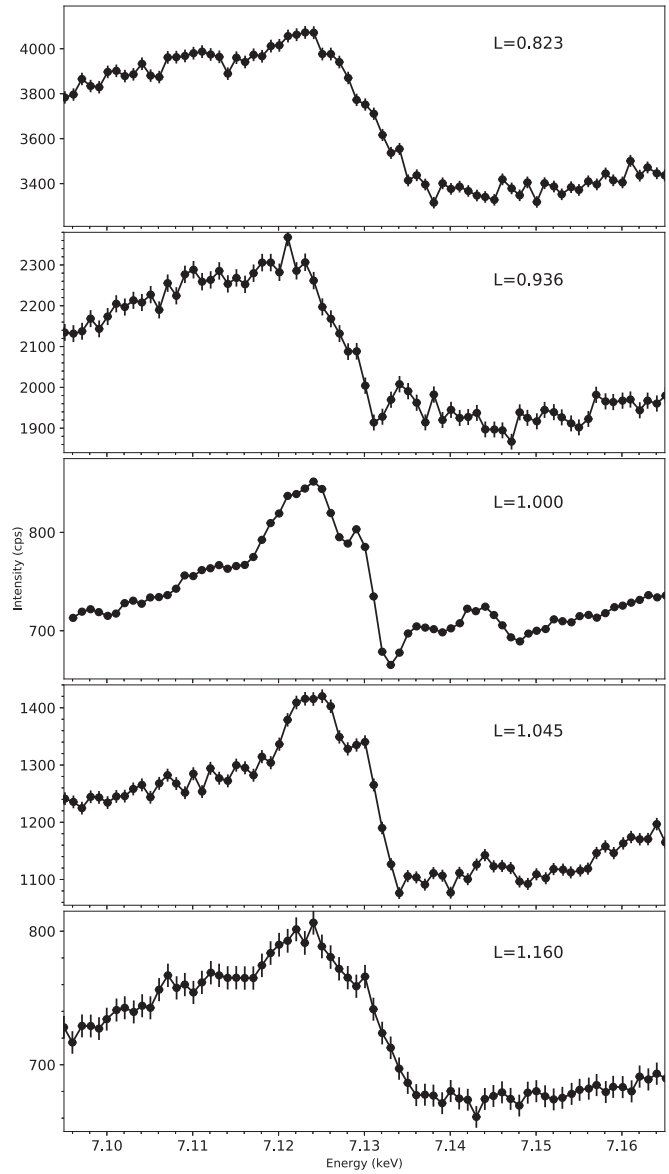

FIG. 2. RXD spectra at the (001) position, on the maximum of the two preceding Kiessig fringes, at $L = 0.823$ and $L = 0.936$, and on the two next at $L = 1.045$ and $L = 1.16$ (see Fig. 1), $T = 40$ K.

We sought the $(002n + 1)$ reflections whose RXD spectra in bulk are a direct probe of the charge-density modulation along H = (001) [10,12]. Scaling with intensities reported for the bulk reflections [16] to the present UTF (004) intensity, the UTF (005) and (001) reflections would be expected at 200 counts/s, which is about the actual background count rate at the (005) position, and 10 counts/s, about two orders of magnitude smaller than the present CTR. Near the (005) position, a fringe can be seen; its RXD signal has some resemblance to the bulk (005) but its count rate was too low and noisy to be fully exploited. We thus took advantage of the strong CTR from the substrate as it appears modulated by interference with the film, thereby boosting its signal. Figure 2 shows several RXD spectra on fringes maxima around and on the (001) position *dip*, where we found an intense signal from the film, and remarkably structured at 40 K. The intensity being the squared amplitude

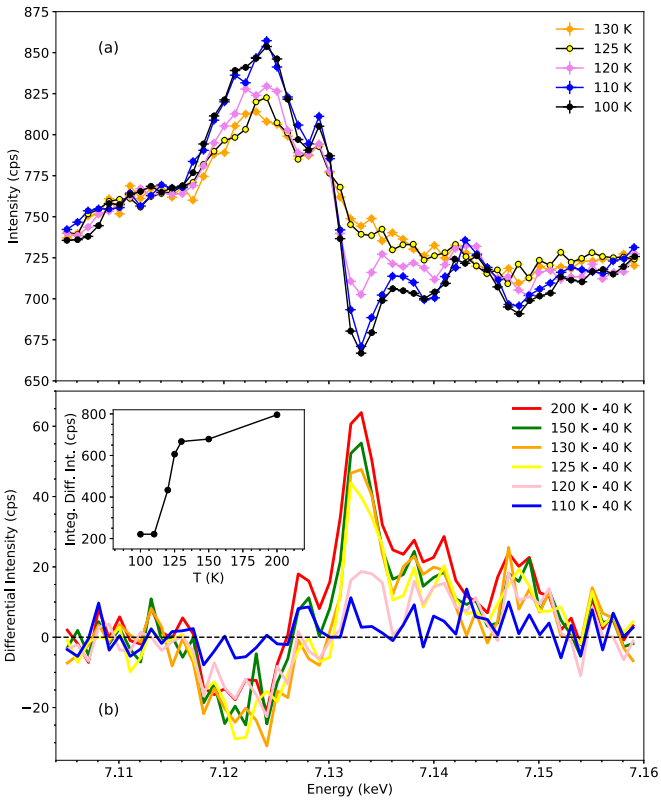

FIG. 3. (a) Temperature evolution of spectra taken at $Q = (001)$, evolving strongly around 120 K. Spectra are scaled to the 40 K data at 7.1 eV to correct for Debye-Waller decrease of intensity (e.g., scan at 200 K is multiplied by 1.14). (b) The 40 K data are subtracted to all the data, isolating the differential spectroscopic signal, resulting in statistical noise around zero at 100 K, and maximum signal at 200 K (red thick line) (inset). Differential intensities $|I(T) - I(40\text{ K})|$ integrated over the whole energy range and plotted against the temperature.

of the total structure factor $F = F_{\text{cap}} + F_{\text{film}} + F_{\text{sub}}$, we deduce from all these observations that the signal at the (001) position is governed by $|F_{\text{sub}}|^2 + 2\text{Re}(F_{\text{sub}}F^*_{\text{film}})$, where the terms with the cap layer are taken out because of roughness, as well as the film alone, which appears relatively too weak to give a Bragg reflection.

We then went on heating the sample from 40 K, measuring the spectra at $Q = (001)$. Figure 3(a) shows several (001) RXD spectra showing an abrupt change near 120 K. The spectra were scaled together below the edge to correct for a slight Debye-Waller damping. Figure 3(b) shows the differential scans consisting of subtracting the scan at 40 K from those measured at 100, 110, 120, 125, 130, 150, and 200 K. This temperature sampling provides a resolution of 5 K (finer sampling would have been time consuming with a 60 s counting time for each energy point). This procedure removes T-independent backgrounds (e.g., fluorescence). The inset in Fig. 3(b) shows the results of integrating the modulus of the differential scans over the energy axis. The sharp transition is evident; we estimate T_V at the steepest slope to be close to 120 ± 5 K. Noteworthy, while we found that below T_V the spectra superposed at 40, 100, and 110 K, we found that, above T_V, there is still a significant intensity continuously adding up, especially near 7133 eV, up to the highest measured temperature at 200 K.

III. DISCUSSION

These spectra can be interpreted by comparison with data published on bulk magnetite. There is a striking resemblance between the reported bulk (005) RXD spectrum Fig. 7 in Ref. [16] and the UTF (001) differential intensity in Fig. 3, but it does not match the reported bulk (001) RXD spectra [16]. The bulk (001) RXD spectra had little Thomson scattering to interfere with, and therefore the absolute square of the resonant signal was dominating the data, whereas here, that same signal interferes with the Thomson scattering from the Ag substrate [we thus find a better correspondence by squaring the present spectrum (not shown)]. The polarization of the scattering can also be discussed. RXD studies usually account for the polarization final state compared to its initial state, giving useful information on the atomic state [17]. The bulk $Q = (001)$ scattering was reported unrotated, thus in the $\sigma \rightarrow \sigma$ channel [16]. Here, the resonant part of the signal is also necessarily in the $\sigma \rightarrow \sigma$ channel because the interference with the Thomson scattering acts as a polarization analyzer tool: only the same initial and final polarization state path can interfere. Overall, we consider that the equivalence of the spectral features already warrant the same conclusion than in the bulk material, that is, the UTF undergoes a charge modulation transition. Here, this magnetite UTF sample on Ag(001) has T_V still near 120 K, which is remarkably close to the bulk value.

To gain better understanding, we performed simulations using the FDMNES code [18]. This code, extensively used for x-ray absorption near edge structure and resonant x-ray scattering has been recently extended to SRXD [19]. The calculation follows the formalism of surface x-ray diffraction [14], but with first-principles calculation of the atomic scattering factors for all the resonant atoms embedded in the unit cell. We have included the Ag(001) substrate, the magnetite film, and the gold cap layer where interfaces are just the juxtaposition of the layers, disregarding intermixing, reconstruction, or segregation. We use a kinematical description, considering that the main region of interest is relatively far from dynamical effects well above the critical angle. In this framework, the substrate has a CTR structure factor [20]. To get the agreement shown in Fig. 4, we used a 30 Å gold cap thickness but with a 0.2 occupancy rate and a 20 Å roughness. The average interlayer distance between the topmost magnetite layer and the bottommost gold layer is 2.5 Å. To describe the magnetite film, we used a simple periodical model, 71.2 Å thick at 2.5 Å from the Ag substrate and with a 2 Å roughness at the interface with gold. To account for the tetrahedral distortion from the RT bulk magnetite cubic structure, we have used the actual unit cell parameters, with the same atom positions in reduced unit. This was done for both the RT and low temperature (LT) phases. We used the RT structure and the LT *Pmca* structure proposed by Wright *et al.* [6], sufficiently precise in this context. Two simulations were performed, with and without a charge modulation, in the same LT structure. To do so, we relied on our previous study

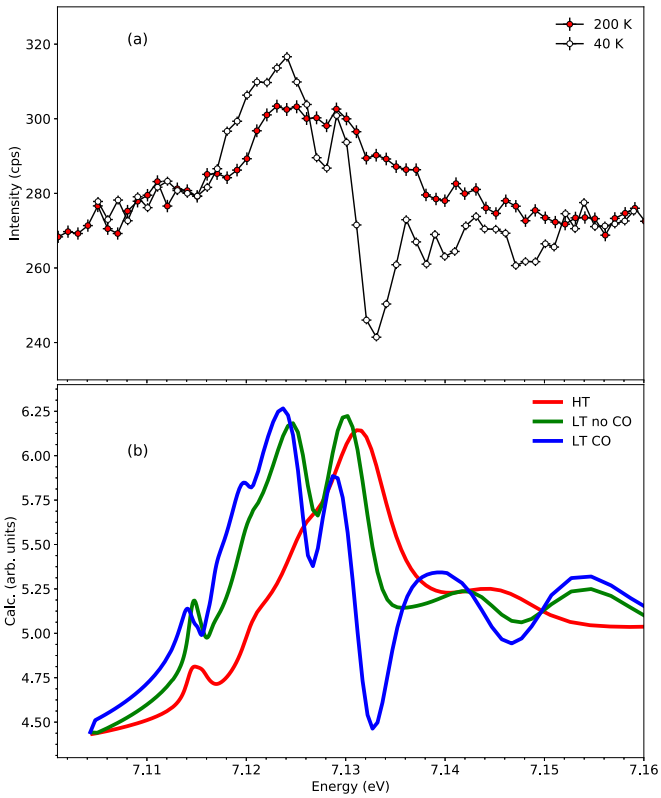

FIG. 4. (a) $Q = (001)$ RXD spectra measured at 40 K and 200 K with a smaller detector area but better Q resolution than in Fig. 3, and negligible fluorescence, also scaled for Debye-Waller damping, to be compared to (b) calculated spectra for the LT structure with (CO) and without (no CO) a chemical shift, and with the high temperature (HT) structure. Spectra are scaled together for comparison and the energy scale of the simulations was shifted so that the dip of the LT data is aligned with the calculated CO spectra at 7.133 keV.

[10], where we found that a $\pm 0.2\ e^-$ charge difference on two octahedral Fe site translates to a ± 0.2 eV shift on their scattering factors. The comparison with the data in Fig. 4 reinforces the interpretation that a charge disproportionation is observed at (001) propagation vector similar to the bulk. With these simulations in hand, the scattering interference with the substrate provides information on the actual stacking of the Fe species. The procedure is similar to techniques measuring phase information by interfering with a known reference to retrieve the sign of magnetic couplings [21] or absolute structures [22], for instance. A precise description of the Magnetite-Ag interface is out of reach at the present stage. Nevertheless, the diffracted intensities strongly depend on the interference between the Ag substrate and the magnetite thin film. The phase difference between these two scatterers is determined not only by their interlayer distance but also by the choice of the very first interfacial atomic layer of the magnetite film. All the rest of the magnetite slab is then supposed, built following a perfect ordering and, consequently, the topmost magnetite layer depends on this choice and of course on the thickness. We have used this sensitivity to determine which of the intraunit cell planes better fit the spectra. We found a nonambiguous agreement when the interface corresponds to a layer of octahedral Fe, in comparison with the layers of tetrahedral Fe or O atoms.

The data above 125 K have unexpected line shapes. For one, there is still a signal at the Fe edge [Fig. 4(a)], evidencing that Fe atoms contribute to the reflection despite being a forbidden reflection in the bulk above T_V due to translational symmetry within the unit cell. The film being not complete, we might see here some Fe scattering because of the incomplete .75 unit cell (as reproduced in the simulations); roughness would have a similar effect. An analogous finding was reported in the system $NdNiO_3$ [23], where it was explained by remnant octahedral distortions and tilts of the Ni site, leading to a tensorial scattering factor at the resonance. Here, the bulk RT structure is probably not established because of the strain; the actual space group would have a lower symmetry than in the bulk. In this regard, the continuous evolution from T_V to 200 K is intriguing [Fig. 3(b)]. The current simulations of the spectra with the LT structure *without* the charge ordering seem to better reproduce the spectra at 200 K. The scenario would be that part of the atomic structure already evolves from 200 K until the electronic and atomic structures freeze below T_V. However, crystallographic and RXS studies are needed to be conclusive on this behavior.

IV. CONCLUSION

In conclusion, we have detected the Verwey transition in a magnetite UTF grown on Ag. A strong enhancement of the signal is obtained thanks to the substrate CTR that also acts as a reference scatterer allowing the determination of the Fe stacking at the interface and determination of the $\sigma \rightarrow \sigma$ scattering channel. The transition is rather sharp, near 120 ± 5 K, remarkably close to the bulk T_V compared to UTF on other substrates. We also detected a signal smoothly evolving at least up to 200 K that we interpret as thermal evolvement of the structure anticipating the Verwey transition, whereas both atomic and electronic structures completely freeze below T_V. This finding opens the question on the actual crystallographic structure in which the electronic transition occurs as compared to the bulk structure. Our original methodology was based on resonant x-ray scattering at a single point of the reciprocal space where CTR from the substrate interferes with the thin-film scattering.

ACKNOWLEDGMENTS

This work has been carried out using instruments of the QMAX Project No. ANR-09-NANO-031 funded by the French National Agency (ANR) in the frame of its 2009 programme in Nanosciences, Nanotechnologies and Nanosystems (P3N2009). The LANEF framework (ANR-10-LABX-51-01) is acknowledged for its support with mutualized infrastructure. We acknowledge the ESRF and the French Collaborating Research Group (CRG) for provision of synchrotron radiation facilities. We thank Sébastien Pairis for his assistance in this project.

[1] M. Zając, K. Freindl, T. Ślezak, M. Ślezak, N. Spiridis, D. Wilgocka-Ślezak, and J. Korecki, Thin Solid Films **519**, 5588 (2011).
[2] A. Lamirand, S. Grenier, V. Langlais, A. Ramos, H. Tolentino, X. Torrelles, and M. De Santis, Surf. Sci. **647**, 33 (2016).
[3] X. Liu, C.-F. Chang, A. D. Rata, A. C. Komarek, and L. H. Tjeng, NPJ Quantum Mater. **1**, 16027 (2016).
[4] E. J. W. Verwey, Nature **144**, 327 (1939).
[5] M. Iizumi, T. F. Koetzle, G. Shirane, S. Chikazumi, M. Matsui, and S. Todo, Acta Crystallogr. Sect. B **38**, 2121 (1982).
[6] J. P. Wright, J. P. Attfield, and P. G. Radaelli, Phys. Rev. Lett. **87**, 266401 (2001).
[7] M. S. Senn, J. P. Wright, and J. P. Attfield, Nature **481**, 173 (2012).
[8] M. S. Senn, J. P. Wright, J. Cumby, and J. P. Attfield, Phys. Rev. B **92**, 024104 (2015).
[9] G. Subías, J. García, J. Blasco, M. Grazia Proietti, H. Renevier, and M. Concepción Sánchez, Phys. Rev. Lett. **93**, 156408 (2004).
[10] E. Nazarenko, J. E. Lorenzo, Y. Joly, J. L. Hodeau, D. Mannix, and C. Marin, Phys. Rev. Lett. **97**, 056403 (2006).
[11] Y. Joly, J. E. Lorenzo, E. Nazarenko, J.-L. Hodeau, D. Mannix, and C. Marin, Phys. Rev. B **78**, 134110 (2008).
[12] G. Subías, J. García, J. Blasco, J. Herrero-Martín, M. C. Sánchez, J. Orna, and L. Morellón, J. Synchrotron Radiat. **19**, 159 (2012).
[13] U. Staub, G. I. Meijer, F. Fauth, R. Allenspach, J. G. Bednorz, J. Karpinski, S. M. Kazakov, L. Paolasini, and F. d'Acapito, Phys. Rev. Lett. **88**, 126402 (2002).
[14] I. K. Robinson, R. T. Tung, and R. Feidenhans'l, Phys. Rev. B **38**, 3632 (1988).
[15] E. D. Specht and F. J. Walker, Phys. Rev. B **47**, 13743 (1993).
[16] S. R. Bland, B. Detlefs, S. B. Wilkins, T. A. W. Beale, C. Mazzoli, Y. Joly, P. D. Hatton, J. E. Lorenzo, and V. A. M. Brabers, J. Phys.: Condens. Matter **21**, 485601 (2009).
[17] V. E. Dmitrienko, K. Ishida, A. Kirfel, and E. N. Ovchinnikova, Acta Crystallogr. Sect. A **61**, 481 (2005).
[18] O. Bunău and Y. Joly, J. Phys.: Condens. Matter **21**, 345501 (2009).
[19] Y. Joly, A. Abisset, A. Bailly, M. De Santis, F. Fettar, S. Grenier, D. Mannix, A. Y. Ramos, M.-C. Saint-Lager, Y. Soldo-Olivier, J.-M. Tonnerre, S. A. Guda, and Y. Gründer, J. Chem. Theory Comput. **14**, 973 (2018).
[20] I. K. Robinson, Phys. Rev. B **33**, 3830 (1986).
[21] V. Dmitrienko, E. N. Ovchinnikova, S. P. Collins, G. Nisbet, G. Beutier, Y. O. Kvashnin, V. V. Mazurenko, A. I. Lichtenstein, and M. I. Katsnelson, Nat. Phys. **10**, 202 (2014).
[22] I. McNulty, J. Kirz, C. Jacobsen, E. H. Anderson, M. R. Howells, and D. P. Kern, Science **256**, 1009 (1992).
[23] Y. Lu, A. Frano, M. Bluschke, M. Hepting, S. Macke, J. Strempfer, P. Wochner, G. Cristiani, G. Logvenov, H.-U. Habermeier, M. W. Haverkort, B. Keimer, and E. Benckiser, Phys. Rev. B **93**, 165121 (2016).